Journal of Applied Polymer Science

Enhanced Mechanical Properties and Bactericidal Activity of Polypropylene Nanocomposite with Dual-Function Silica–Silver Core-Shell Nanoparticles

Phansiri Suktha,[1] Kannika Lekpet,[1] Patcharaporn Siwayaprahm,[2] Montree Sawangphruk[1,3]

[1]National Center of Excellence for Petroleum, Petrochemicals and Advance Material, Department of Chemical Engineering, Faculty of Engineering, Kasetsart University, Bangkok 10900, Thailand

[2]Department of Microbiology, Faculty of Science, Kasetsart University, Bangkok 10900, Thailand

[3]Center for Advanced Studies in Nanotechnology and its Applications in Chemical, Food, and Agricultural Industries, Kasetsart University, Bangkok 10900, Thailand

Correspondence to: M. Sawangphruk (E-mail: fengmrs@ku.ac.th)

ABSTRACT: Dual-function silica–silver core-shell (SiO_2@Ag) nanoparticles (NPs) with the core diameter of 17 ± 2 nm and the shell thickness of about 1.5 nm were produced using a green chemistry. The SiO_2@Ag NPs were tested *in vitro* against gram-positive *Staphylococcus aureus* (*S. aureus*) and gram-negative *Escherichia coli* (*E. coli*), both of which are human pathogens. Minimal inhibitory concentrations of the SiO_2@Ag NPs based on Ag content are 4 and 10 $\mu g\ mL^{-1}$ against *S. aureus* and *E. coli*, respectively. These values are similar to those of Ag NPs. SiO_2@Ag NPs were for the first time incorporated to a commodity polypropylene (PP) polymer. This yielded an advanced multifunctional polymer using current compounding technologies i.e., melt blending by twin-screw extruder and solvent (toluene) blending. The composite containing 5 wt % SiO_2@Ag NPs (0.05 wt % Ag) exhibited efficient bactericidal activity with over 99.99% reduction in bacterial cell viability and significantly improved the flexural modulus of the PP. Anodic stripping voltammetry, used to investigate the antibacterial mechanism of the composite, indicated that a bactericidal Ag^+ agent was released from the composite in an aqueous environment. © 2012 Wiley Periodicals, Inc. J. Appl. Polym. Sci. 128: 4339–4345, 2013

KEYWORDS: functional composites; antibacterial; nanocomposites; polymers; nanoparticles; polypropylene; core shell

Received 2 July 2012; accepted 25 September 2012; published online 25 October 2012

DOI: 10.1002/app.38649

INTRODUCTION

Inorganic nanoadditives are currently of interest and widely used in the plastic industries.[1–4] They can enable formulation of new functional nanocomposites with superior properties when compared with the pure commodity plastics, which normally have a limited range of useful properties. For example, incorporating fumed SiO_2 NPs to PP enhances its gas barrier properties.[2] PP filled with powdered SiO_2 NPs can be used to enhance mechanical properties.[5] Ag NPs incorporated into polymers (i.e., polyamide and PP) form high antibacterial nanocomposites.[6–8] This can play an important role in the manufacture and use of medical devices, appliances, filters, nonwoven films, and antibacterial food packaging films.[9,10] Such materials have high temperature stability, low volatility,[11] and can thereby be used to prevent bacterial infections.[4]

SiO_2-Ag core shell (SiO_2@Ag) NPs have attracted much interest due to their unique and multifunctional properties as well as their potential applications in catalysis, biosensor, optical devices and medical imaging.[12,13] There are many methods used to produce SiO_2@Ag NPs. These include an electroless deposition,[14,15] a sol-gel method,[16–18] and a seed-mediated growth technique.[19,20] Recently, we reported a facile and green chemistry synthesis of SiO_2@Ag NPs for hydrogen peroxide detection.[12] The growth mechanism of the SiO_2@Ag NPs was that Ag^+ was initially bound to the surfaces of colloidal SiO_2 nanospheres by electrostatic interaction to form an Ag^+ layer.[12,21,22] Then, Ag^+ was reduced to Ag metal by a green and mild reducing agent (D-(+)-glucose).[12] To the best of our knowledge, SiO_2@Ag NPs have not yet been incorporated to PP. In this work, we then introduced SiO_2@Ag NPs produced using the green chemistry synthesis[12] for improving both mechanical properties and bactericidal activity of PP nanocomposites.

EXPERIMENTAL

Chemicals and Materials

All analytical grade chemicals were used as received without further purification. These chemicals were tetraethyl orthosilicate

(TEOS, 98 wt %, Acros), methanol (99.9 v %, Merck), ammonium hydroxide (30 v%, Mallinckrodt), silver nitrate (99.8 wt %, Prolabo), D-(+)-glucose (99.5 wt %, Himedia), potassium chloride (99 wt %, Aldrich), nitric acid (70 v %, Aldrich), PP homopolymer plastic resin (99 wt %, IRPC), poly(propylene-*graft*-maleic anhydride) (PP-*g*-MA, average $M_w \sim 9100$, average $M_n \sim 3900$, maleic anhydride 8–10 wt %, Aldrich). Glassy carbon electrodes were obtained from Metrohm Autolab.

Preparations of SiO_2 and SiO_2@Ag NPs

Preparation methods of SiO_2 and SiO_2@Ag NPs were previously reported in detail.[12] Briefly, monodispersed 6 wt % SiO_2 NPs with diameter of 17 ± 2 nm were first obtained by a modified Stöber method.[23] SiO_2 precursor, 22 mL TEOS, was added to methanol solvent (77 mL) with mixing by a magnetic stirrer at 300 rpm. Subsequently, Milli-Q water (7.2 mL) was added to the solution and the pH of the mixture was adjusted to 9 using NH_4OH (0.8 mL) and further stirred for 30 min. The mixture was left at a static condition and ambient temperature overnight. To prepare SiO_2@Ag NPs, an aqueous solution of $AgNO_3$ was added to the colloidal suspension of SiO_2 NPs while mixing on a magnetic stirrer at 300 rpm. After 30 min, D-(+)-glucose was added to the mixture and heated to 50°C ± 2°C. The mole fraction ratio of SiO_2 : Ag : D-(+)-glucose was 100 : 1 : 1. The structural and morphology of all as-prepared NPs characterized by X-ray diffraction (XRD), dynamic light scattering (DLS), energy-dispersive X-ray spectroscopy (EDX), and transmission electron microscopy (TEM) of the materials were previously reported.[12]

Preparations of SiO_2@Ag NPs/PP Nanocomposites

SiO_2@Ag NPs/PP-Coated Glass Slides for Antibacterial Tests. SiO_2@Ag/PP nanocomposites were prepared using a solvent blending method. The SiO_2@Ag NPs were loaded to the PP matrix with different SiO_2@Ag contents (0.1–5.0 wt % SiO_2 and 0.001–0.05 wt % Ag) as compared with the total mass of the nanocomposites. PP-*g*-MA, a compatibilizer, was used to assist the dispersion of core-shell NPs in the PP matrix. The mole fraction of PP-*g*-MA to the core-shell NPs was fixed at 2 : 1. A known quantity (1 g) of PP granules was added to 25-mL toluene with continuous stirring (300 rpm) at 120°C until the PP was completely dissolved. Then, SiO_2@Ag NPs and PP-*g*-MA were added into the aforementioned polymer solution. This mixed solution was stirred for 30 min then ultrasonicated for 5 min to attain better dispersion of NPs in the polymer matrix. A glass slide (2.5 × 7.5 cm^2) was immersed into the composite for 4 h at ambient temperature. This yielded a nanocomposite film. The as-prepared nanocomposite film was then used for antibacterial testing.

SiO_2@Ag NPs/PP Nanocomposites for Mechanical Tests. Nanocomposites containing SiO_2@Ag NPs at 5 wt % SiO_2 and 0.05 wt % Ag were prepared by melt mixing in a Lab-Tech twin-screw co-rotating extruder with *L*/*D* 40 (D26 mm). Note that the 5 wt % SiO_2 loading was previously reported as an optimum condition for the SiO_2/PP nanocomposites.[2,5] To improve the dispersion of NPs in the PP matrix, 10 wt % PP-*g*-MA was used as a compatibilizer and the residence time of the mixture in the mixing section was increased after feeding NPs. The apparatus had a vacuum venting port to remove any volatile products formed during the compounding process. Before melt processing, core-shell NPs were mixed with PP pellets and dried for 24 h at 105°C to remove the remaining traces of impurities. The mixed NP/PP pellets were then fed into the throat of a twin screw pelletizing extruder. Compounding was done using a screw rotating speed of 200 rpm and a temperature profile of 185, 195, 200, 200, 200, 195, and 185°C in the sequential heating zones from the hopper to the die. After compounding, the material was extruded from a die having three cylindrical nozzles of 4-mm diameter to produce cylindrical extrudates. These were immersed immediately in a water bath (22°C) and pelletized into 5-mm pellets with an adjustable rotating knife located after the water bath.

Antibacterial Activity Tests

The antibacterial activity tests were carried by following a standard testing method.[24] The NPs dispersed in methanol were collected by centrifugation, washed three times with water, and resuspended in water by ultrasonication for 10 min. The suspended NPs were then used for antibacterial testing against both gram-negative *E. coli* and gram-positive *S. aureus*. These bacteria were selected because they are both well-known pathogenic bacteria responsible for foodborne illnesses and clinical infections. The bacterial cells were initially prepared for the antibacterial testing of the as-prepared core-shell samples. *E. coli* and *S. aureus* were streaked on nutrient agar (NA) plates to separate bacterial cells to single colonies and incubated for overnight at 37°C. Microorganisms from a single colony of each type of bacteria were used to inoculate 5 mL of sterile nutrient broth (NB) medium in test tubes. Inoculated media was incubated on a shaker (150 rpm) for 24 h at 37°C. Optical density of media at a wavelength of 0.6 μm ($OD_{0.6}$) was then measured. Cells were allowed to grow on the shaker incubator until $OD_{0.6}$ reached 0.4. After bacterial cells were ready for use in antibacterial testing of the core-shell NPs, the test was begun by exposing bacterial cells [10^8 colony forming units (CFU) per mL] to the minimum inhibitory concentration (MIC) of Ag. This cell number was selected since it represents a mid-range value of the logarithmic growth phase. A dilution plating technique was used to determine the number of viable cells remaining after 10-min treatment. Surviving cells plated onto NA and incubated for 24 h at 37°C. Dilutions were done by adding 0.1 mL of the original bacterial solution to 0.9 mL of sterile water. The resulting solution was subsequently diluted until viable colonies could be counted. To ensure that any reduction in bacterial cells was due to the core-shell NPs, the observed results were compared to the results obtained by treating bacteria with the SiO_2 alone i.e., no Ag and two control experiments: (i) with the absence of both bacteria and NPs (negative control) and (ii) with the presence of bacteria and no core-shell NPs treatment (positive control). All antibacterial tests of the core-shell NPs were repeated for five times and the mean values were reported.

In addition, the antibacterial activity of SiO_2@Ag NPs/PP nanocomposites containing the Ag contents of 0, 0.001, 0.010, 0.025, and 0.050 wt % coated on glass slides was tested using a modified standard method.[25] In this test, 100 μL of bacterial suspension in saline at $OD_{0.6}$ ≈0.4 were placed onto the as-prepared

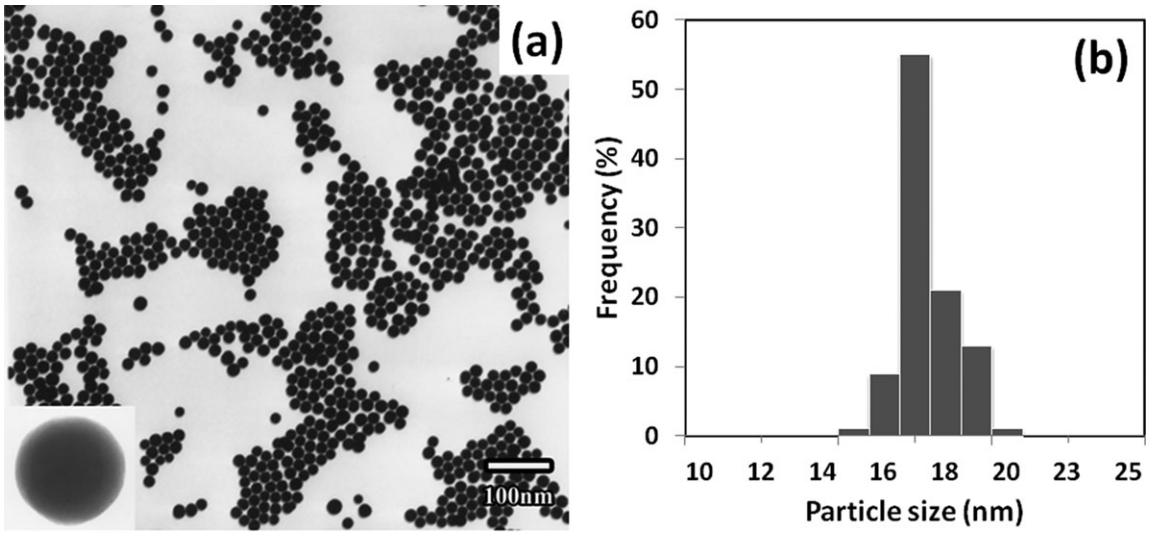

Figure 1. (a) Transmission electron micrograph of SiO_2 NPs including an inset image of a single SiO_2 NP and (b) the size distribution of SiO_2 NPs.

glass slide in a fume hood. After drying in air, the resulting slide was placed in a Petri dish, immediately covered with fresh NA medium, and incubated at 37°C overnight. Viable cells were counted using standard dilution plating. A control experiment i.e., using an uninoculated PP-coated glass slide was also done. All antibacterial tests of the nanocomposites were repeated for five times and the mean values were reported.

Anodic Stripping Voltammetry Measurement

First, the as-prepared nanocomposite film coated glass slide was stored in a flask containing 100 mL aqueous media (93-mL distilled water + 7 mL 0.1*M* HNO_3) at ambient temperature for 1 week. This was previously reported as an appropriate soaking time for Ag/PP composite since no sudden increase in Ag^+ release was observed from the 7th day onwards.[26] HNO_3 was added to prevent the released Ag^+ ions from reducing to metallic silver. Second, electrodeposition of the reducible species (Ag^+) onto glassy carbon electrode surfaces was carried out at a constant potential (-0.1 V vs. Ag/AgCl) using a chronoamperometry. Third, electrooxidation (stripping) of reduced Ag metal by applying an anodic potential was done to bring metallic Ag back into solution (Ag^+). Anode stripping voltammetry (ASV) was then used to measure trace amounts of Ag^+ released from the SiO_2@Ag NPs/PP nanocomposite. In a typical ASV measurement, coated glassy carbon, Ag/AgCl, and Pt wire were used as working, reference, and counter electrodes, respectively. Experiments were done using a μAUTOLABIII potentiostat (Eco-Chemie, Utrecht, Netherlands). The supporting electrolyte used was 0.1*M* $NaNO_3$.

Measurements of Mechanical Properties

The specimens for mechanical property tests were prepared in an Engel single screw injection molding machine (Monomat 80, Germany). This machine consists of three different heating zones and the temperatures of these were 245, 195, and 190°C for the feeding zone, compressing zone, and metering zone,

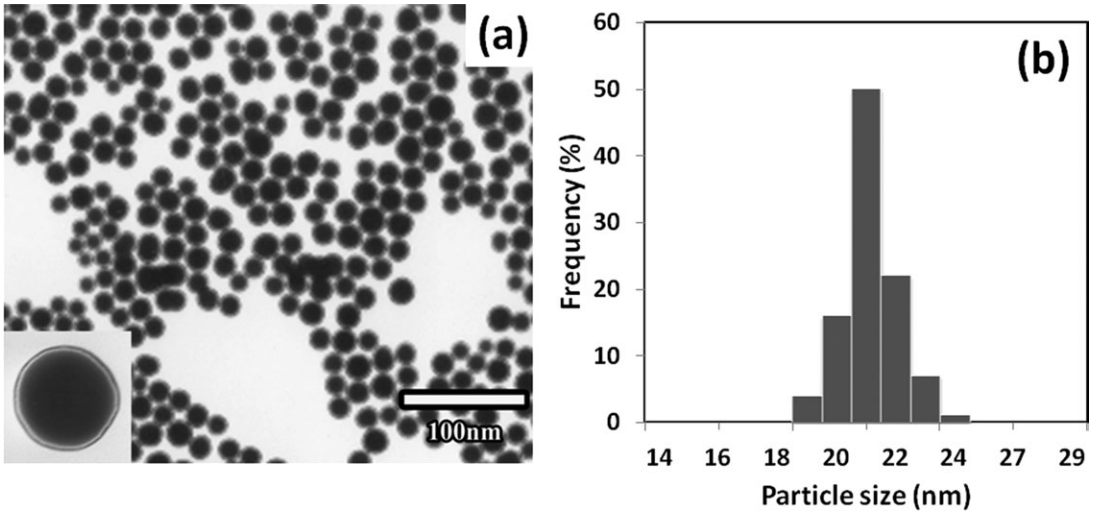

Figure 2. (a) Transmission electron micrograph of SiO_2@Ag NPs including an inset image of a single SiO_2@Ag NP and (b) the size distribution of SiO_2@Ag NPs.

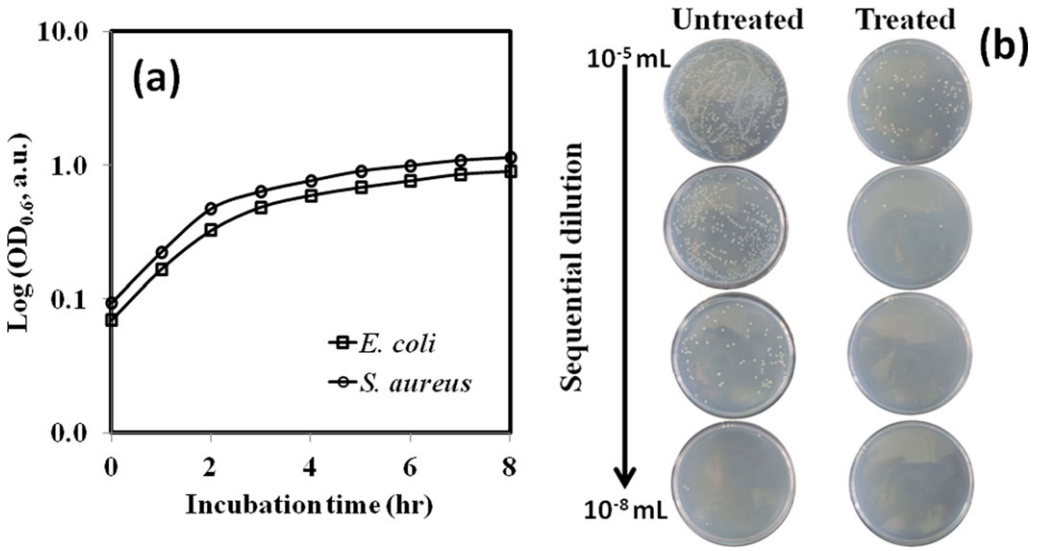

Figure 3. (a) Growth curves of *E. coli* and *S. aureus* and (b) photographs of surviving *S. aureus* colonies untreated (left) and treated (right) by SiO_2@Ag NPs on the sterile plates with sequential dilutions of 10^{-5}–10^{-8}. [Color figure can be viewed in the online issue, which is available at wileyonlinelibrary.com.]

respectively. The mold was cooled with water at 25°C. The tensile properties were investigated using ASTM D638 on samples with the dimensions of 15 cm × 1.9 cm × 0.3 cm (length × width × thickness). The testing apparatus was a universal testing machine (UTM, Hounsfield) at a cross-head speed of 5 mm min^{-1}. Flexural testing was conducted on the same machine according to ASTM D790 with a three-point bending system. Samples with dimensions of 15 cm × 15 cm × 0.3 cm were tested at a cross-head speed of 2.0 mm min^{-1}. Five specimens were tested for each set of samples, and the mean values were reported. Tensile and flexural toughness were calculated from the area under stress–strain curve.

RESULTS AND DISCUSSION

Characterizations of SiO_2 and SiO_2@Ag NPs

The TEM image in Figure 1(a) shows dispersed SiO_2 NPs. Average diameter of SiO_2 NPs is 17 ± 2 nm as determined from the size histogram [Figure 1(b)]. The inset magnified image of a single nanosphere of SiO_2 in Figure 1(a) represents a condition with no shell on the surface of SiO_2. SiO_2@Ag NPs [Figure 2(a)] are also highly dispersed and rather uniform. The particle size histogram [Figure 2(b)] shows their average diameter as 21 ± 2 nm. The inset image shows the average shell thickness is about 1.5 nm. The XRD, EDX, and DLS characteristics of as-prepared NPs as well as the mechanism of the core-shell growth was previous reported.[12]

Bactericidal Activities

SiO_2 and SiO_2@Ag NPs. *E. coli* and *S. aureus* were selected for testing antibacterial activity of SiO_2@Ag NPs. At $OD_{0.6}$ ≈0.4, bacterial cells were in the middle portion (about 2 h) of their logarithmic growth phase as determined from their growth curves [Figure 3(a)]. Viable cells treated with core-shell NPs and incubated at 37°C for 24 h were counted by a dilution plating method. Photographs of plates were made from sequential dilutions (10^{-5}–10^{-8} mL) viable *S. aureus* colonies. These samples were untreated with core-shell NPs and their controls then grown on sterile plates. They are shown in Figure 3(b). Inhibition of *S. aureus* growth after treating with SiO_2@Ag NPs was clearly observed. Surviving *S. aureus* colonies could be counted when samples were diluted to 10^{-5} mL. Untreated bacteria could be counted at a dilution of 10^{-8}. This represents three orders of magnitude difference, indicating that the SiO_2@Ag NPs have considerable antibacterial activity.

For further quantitative analyses, several calculations were done. N/N_0 was determined, where the term N_0 denotes the number

Table I. Viability, N/N_0, and % Reduction in Viability of *E. coli* and *S. aureus* Cultures After Treatment with SiO_2@Ag NPs at Minimal Inhibitory Concentrations (MICs) based on Ag Contents (10 μg mL^{-1} for *E. coli* and 4 μg mL^{-1} for *S. aureus*)

	Viability (CFU mL^{-1})		N/N_0		% Reduction in viability	
Samples	*E. coli*	*S. aureus*	*E. coli*	*S. aureus*	*E. coli*	*S. aureus*
Negative control	0	0	N/A	N/A	N/A	N/A
Positive control	567000000	581000000	1.00	1.00	0.00	0.00
SiO_2 NPs	552000000	571000000	0.97	0.98	2.65	1.72
SiO_2-Ag core-shell NPs	15722333	131000000	0.03	0.23	97.23	77.45

Table II. Viability, N/N_0, and % Reduction in Viability of *E. coli* and *S. aureus* Cells After Being Cultured on SiO_2@Ag NPs/PP Nanocomposites at Different Ag Loadings

	Viability (CFU mL^{-1})		N/N_0		% Reduction in viability	
Ag loading (wt %)	*E. coli*	*S. aureus*	*E. coli*	*S. aureus*	*E. coli*	*S. aureus*
0	432200000	370000000	1.00	1. 00	0.00	0.00
0.001	255166667	236166667	0.59	0.64	40.96	36.17
0.010	140166667	125333333	0.32	0.34	67.57	66.13
0.025	80666667	73333333	0.19	0.20	81.34	80.18
0.050	48000	50000	0.00	0.00	99.99	99.99

of CFU at the beginning of the treatment before adding the SiO_2@Ag NPs (time 0) and N is the number of CFU after treatment with the NPs at MICs (10 $\mu g\ mL^{-1}$ for *E. coli* and 4 $\mu g\ mL^{-1}$ for *S. aureus*). The % reduction in viability was determined (% reduction = $(A - B)/A \times 100$). In this calculation, A is the number of surviving microbial colonies in the blank solution and B is the number of surviving microbial colonies in the SiO_2@Ag NPs. Results are given in Table I. All data listed were determined from three replicate experiments. The results show that SiO_2 NPs dispersed in water are not good for inhibiting the cell growth of *E. coli* and *S. aureus* since % reductions in cell viability are only 2.65 and 1.72 for *E. coli* and *S. aureus*, respectively (see Table I). However, SiO_2 with the Ag shell can significantly inhibit *E. coli* and *S. aureus* cells when treated with SiO_2@Ag NPs at MICs of 10 and 4 $\mu g\ mL^{-1}$, respectively. *E. coli* and *S. aureus* viability was reduced by 97.23 and 77.45%, respectively. At 10 $\mu g\ mL^{-1}$, no viable *S. aureus* cells were observed. The MICs of the core-shell NPs in this study are similar to those of Ag NPs (3–40 $\mu g\ mL^{-1}$).[27–29] These values are slightly lower than those of Fe_2O_3-SiO_2-Ag composites (16–31 $\mu g\ mL^{-1}$)[30] and considerably lower than those of metal oxide NPs such as nanocrytalline 8 ± 1 nm MgO (625 $\mu g\ mL^{-1}$).[24] Lower MIC yields better antibacterial activity. The results here indicate that the as-prepared core-shell NPs are able to inhibit *S. aureus* more easily than *E. coli*. This is because the cell membranes of gram-negative *E. coli* consist of an outer layer of lipopolysaccharide and proteins. This outer layer confers protection upon *E. coli* cells and is not found on the cell membranes of gram-positive *S. aureus*. As a result, gram-negative *E. coli* is in general more difficult to inactivate in this manner.[31]

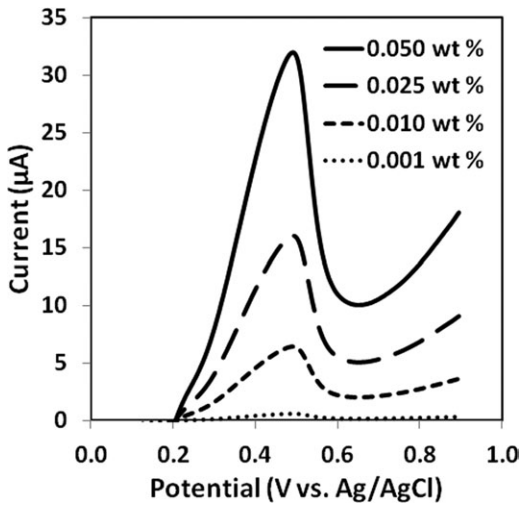

Figure 4. Anodic stripping voltammograms of SiO_2@Ag NPs/PP nanocomposites containing the Ag contents of 0, 0.001, 0.010, 0.025, and 0.050 wt %.

SiO_2@Ag NPs Containing PP Nanocomposites. Polymer nanocomposites were obtained using a solvent blending technique employing the dispersant PP-*g*-MA and coated on the microscope glass slides. The antibacterial activity of SiO_2@Ag NPs/PP nanocomposites was studied using a challenge test.[25] Results showed that increasing the mass loading of the core-shell NPs from 0.001 to 0.05 wt % based on Ag content leads to increased inhibitory activity as shown in Table II. The viable cell counts of both *E. coli* and *S. aureus* were reduced by up to 99.99% at 0.05 wt % of Ag loadings. Untreated PP showed no antibacterial activity. This result is in good agreement with Ag/polyimide nanocomposite with Ag loading of 0.06 wt %.[8] The antibacterial mechanism observed in the composites is possibly due to Ag^+ biocide released from polymer nanocomposites.[8,11]

Silver Ion Release

A typical voltammogram obtained from ASV shows the value of the stripping potential and the peak height and area. These decrease in subsequent stripping scans indicating reflecting decreasing concentration of silver on the glassy carbon electrode surface. The summation of all stripping scans is directly proportional to the total concentration of the silver ions released from the SiO_2@Ag NPs/polypropylene nanocomposites. Figure 4 shows ASVs which are the summation curves of all the stripping

Table III. Mechanical Properties of PP as well as SiO_2/PP, and SiO_2@Ag NPs/PP Nanocomposites

Mechanical properties	PP	SiO_2/PP	SiO_2-Ag/PP
Flexural modulus (MPa)	1630 ± 10	1850 ± 15	1860 ± 16
Flexural strength (MPa)	48.4 ± 0.4	53.2 ± 0.5	52.4 ± 0.5
Tensile modulus (MPa)	1810 ± 20	1840 ± 23	1830 ± 25
Tensile strength (MPa)	36.8 ± 0.1	36.7 ± 0.2	36.9 ± 0.2

scans for composites with different Ag loading contents. A stripping peak at about 0.5 V vs. Ag/AgCl in Figure 4 is related to oxidation of Ag metal ($Ag \rightarrow Ag^+ + e^-$). This indicates that nanocomposites can release Ag^+ biocide in an aqueous environment. Additionally, the content of released silver increased with the amount of silver incorporated into the composites. These results are in good agreement with previous studies of Ag incorporation into polymer nanocomposites.[8,11,26] Using a calibration method,[8,11,26] the quantitative amount of Ag^+ release can be determined. The concentration of Ag^+ released from the SiO_2@Ag NPs/polypropylene composite is in good agreement with that released from the Ag/PP composite.[26] These composites contained 0.05 wt % Ag with respect to one gram of the solid composite. At lower Ag loading levels, the released Ag^+ was $\sim$ 5.0, 2.2, and 0.4 $\mu g\ L^{-1}$ for loading of 0.025, 0.010, and 0.001 wt %, respectively. Ag^+ released from the SiO_2@Ag NPs/polypropylene nanocomposites in the aqueous environment can inactivate bacterial cells. It binds to tissue proteins of bacteria and causes structural changes in bacterial cell walls and nuclear membranes leading to cell death.[32–34]

Mechanical Testing

The mechanical performance of SiO_2@Ag/PP composites is listed in Table III. The results show that the flexural strength values of SiO_2@Ag/PP and SiO_2/PP composites are 53.2 $\pm$ 0.5 and 52.4 $\pm$ 0.5 MPa while that of the PP is 48.4 $\pm$ 0.4 MPa. The flexural strength values listed in Table III indicate that the capability of the composites to support stress transmitted from the thermoplastic matrix is rather good. In addition to flexural strength, the flexural modulus of the composites is 220–230 MPa higher than that of PP. This shows that stiffness of the composites is good. However, tensile strength and tensile modulus describing the elastic properties of the composites are approximately the same as those of PP. This is in good agreement with previous reports that ungrafted nano SiO_2 NPs cannot improve tensile strength and tensile modulus of PP.[35] This data also indicates that addition of SiO_2@Ag NPs does not cause a reduction in tensile strength. It was previously reported that incorporating pure Ag NPs into polyamide caused reduction in tensile strength of that polymer.[36] This is because metal additives e.g., silver NPs can create cavities in the polymer matrix due to the debonding of the polymer from the metal surface.

CONCLUSIONS

Monodispersed SiO_2 NPs with diameter of 17 $\pm$ 2 nm were successfully obtained by a modified Stöber method. The SiO_2 NPs were then used as a core precursor for obtaining the SiO_2@Ag NPs with the shell thickness of about 1.5 nm under a green chemistry synthesis for which D-(+)-glucose was used as a reducing agent. The antibacterial activities of core-shell NPs and their composites with polypropylene were tested against *S. aureus* and *E. coli*. The minimum inhibitory concentrations based on Ag content of SiO_2@Ag NPs are 4 and 10 $\mu g\ mL^{-1}$ for *S. aureus* and *E. coli*, respectively. These values are in good agreement with those of Ag NPs. SiO_2@Ag NPs incorporated into polypropylene matrices exhibited high antibacterial activity (about 99 % reduction in viability) at Ag loading levels of 0.05 wt %. The flexural strength and modulus of the composite were investigated according to ASTM D638 and D790. The flexural modulus of the composite was improved about 14% when compared with the pure polypropylene while its tensile strength and modulus are not decreased. The SiO_2@Ag NPs obtained in this work might be applied to other manufacture industrial plastics requiring high antibacterial activity.

ACKNOWLEDGMENTS

This work was supported in part by grants from the Kasetsart University Research and Development Institute, the Thailand Research Fund (MRG5480195), the Commission on Higher Education, Ministry of Education ("the National Research University Project of Thailand" and "Postgraduate Education and Research Programs in Petroleum and Petrochemicals and Advanced Materials").

REFERENCES

1. Ozkaraca, A. C.; Kaynak, C. *Polym. Compos.* **2012**, *33*, 420.
2. Vladimirov, V.; Betchev, C.; Vassiliou, A.; Papageorgiou, G.; Bikiaris, D. *Compos. Sci. Technol.* **2006**, *66*, 2935.
3. Damm, C.; Münstedt, H. *Surf. Coat. Technol.* **2008**, *202*, 5122.
4. Silver, S.; Phung, L. T.; Silver, G. *J. Ind. Microbiol. Biotechnol.* **2006**, *33*, 627.
5. Bikiaris, D. N.; Vassiliou, A.; Pavlidou, E.; Karayannidis, G. P. *Eur. Polym. J.* **2005**, *41*, 1965.
6. Damm, C.; Munstedt, H.; Rosch, A. *Mater. Chem. Phys.* **2008**, *108*, 61.
7. Gawish, S. M.; Avci, H.; Ramadan, A. M.; Mosleh, S.; Monticello, R.; Breidt, F.; Kotek, R. *J. Biomater. Sci.* **2012**, *23*, 43.
8. Sanchez-Valdes, S.; Ramirez-Vargas, E.; Ortega-Ortiz, H.; Ramos-Devalle, L. F.; Mendez-Nonell, J.; Mondragon-Chaparro, M.; Neira-Velazquez, G.; Yanez-Flores, I.; Meza-Rojas, D. E.; Lozuno-Ramirez, T. *J. Appl. Polym. Sci.* **2012**, *123*, 2643.
9. Perkas, N.; Shuster, M.; Amirian, G.; Koltypin, Y.; Gedanken, A. *J. Polym. Sci. A* **2008**, *46*, 1719.
10. Ramos, M.; Jiménez, A.; Peltzer, M.; Garrigós, M. C. *J. Food Eng.* **2012**, *109*, 513.
11. Kumar, R.; Münstedt, H. *Biomaterials* **2005**, *26*, 2081.
12. Sawangphruk, M.; Sanguansak, Y.; Suktha, P.; Klunbud, P. *Electrochem. Solid-State Lett.* **2012**, *15*, F5.
13. Jankiewicz, B. J.; Jamiola, D.; Choma, J.; Jaroniec, M. *Adv. Colloid. Interface Sci.* **2012**, *170*, 28.
14. Zhu, M.; Qian, G.; Hong, Z.; Wang, Z.; Fan, X.; Wang, M. *J. Phys. Chem. Solids* **2005**, *66*, 748.
15. Ding, G.; Qian, G.; Wang, Z.; Qiu, J.; Wang, M. *Mater. Lett.* **2006**, *60*, 3335.
16. Jeon, H.-J.; Yi, S.-C.; Oh, S.-G. *Biomaterials* **2003**, *24*, 4921.
17. Akhavan, O.; Azimirad, R.; Moshfegh, A. Z. *J. Phys. D* **2008**, *41*, 195305.
18. Kobayashi, Y.; Katakami, H.; Mine, E.; Nagao, D.; Konno, M.; Liz-Marzan, L. M. *J. Colloid. Interface Sci.* **2005**, *283*, 392.

19. Jiang, Z.-J.; Liu, C.-Y. *J. Phys. Chem. B* **2003**, *107*, 12411.
20. Nischala, K.; Rao, T. N.; Hebalkar, N. *Colloids Surf. B* **2011**, *82*, 203.
21. Pol, V. G.; Srivastava, D. N.; Palchik, O.; Palchik, V.; Slifkin, M. A.; Weiss, A. M.; Gedanken, A. *Langmuir* **2002**, *18*, 3352.
22. Tang, S.; Tang, Y.; Zhu, S.; Lu, H.; Meng, X. *J. Solid State Chem.* **2007**, *180*, 2871.
23. Stöber, W.; Fink, A.; Bohn, E. *J. Colloid Interface Sci.* **1968**, *26*, 62.
24. Makhluf, S.; Dror, R.; Nitzan, Y.; Abramovich, Y.; Jelinek, R.; Gedanken, A. *Adv. Funct. Mater.* **2005**, *15*, 1708.
25. Kumar, A.; Vemula, P. K.; Ajayan, P. M.; John, G. *Nat. Mater.* **2008**, *7*, 236.
26. Radheshkumar, C.; Münstedt, H.,*React Funct Polym* **2006**, *66*, 780.
27. Panacek, A.; Kvitek, L.; Prucek, R.; Kolar, M.; Vecerova, R.; Pizurova, N.; Sharma, V. K.; Nevecna, T.; Zboril, R. *J. Phys. Chem. B* **2006**, *110*, 16248.
28. Sharma, V. K.; Yngard, R. A.; Lin, Y. *Adv. Colloid Interface Sci.* **2009**, *145*, 83.
29. Krishnaraj, C.; Jagan, E. G.; Rajasekar, S.; Selvakumar, P.; Kalaichelvan, P. T.; Mohan, N. *Colloid. Surf. B* **2010**, *76*, 50.
30. Zhang, X.; Niu, H.; Yan, J.; Cai, Y. *Colloid. Surf. A* **2011**, *375*, 186.
31. Xu, K.; Wang, J. X.; Kang, X. L.; Chen, J. F. *Mater. Lett.* **2009**, *63*, 31.
32. Rai, M.; Yadav, A.; Gade, A. *Biotechnol. Adv.* **2009**, *27*, 76.
33. Morones, J. R.; Elechiguerra, J. L.; Camacho, A.; Holt, K.; Kouri, J. B.; Ramirez, J. T.; Yacaman, M. J. *Nanotechnology* **2005**, *16*, 2346.
34. Navarro, E.; Piccapietra, F.; Wagner, B.; Marconi, F.; Kaegi, R.; Odzak, N.; Sigg, L.; Behra, R. *Environ. Sci. Technol.* **2008**, *42*, 8959.
35. Cai, L. F.; Mai, Y. L.; Rong, M. Z.; Ruan, W. H.; Zhang, M. Q. *Express Polym. Lett.* **2007**, *1*, 2.
36. Radheshkumar, C.; Munstedt, H. *Mater. Lett.* **2005**, *59*, 1949.